Marine Pollution Bulletin 211 (2025) 117360

Contents lists available at ScienceDirect

Marine Pollution Bulletin

journal homepage: www.elsevier.com/locate/marpolbul

# Microplastic pollution in salt marsh and urban tributary sediment cores of the River Thames estuary, UK: Spatial and temporal accumulation trends

Megan M. Trusler [a,b], Sarah Cook [c], Barry H. Lomax [b], Christopher H. Vane [a,*]

[a] British Geological Survey, Organic Geochemistry Facility, Keyworth, Nottingham NG12 5GG, United Kingdom
[b] School of Biosciences, University of Nottingham Sutton Bonnington Campus, Loughborough LE12 5RD, United Kingdom
[c] Life Sciences, University of Warwick, Coventry CV4 7AL, United Kingdom

ARTICLE INFO

*Keywords:*
Plastic polymer
London
Urbanisation
Tideway, contamination, anthropocene

ABSTRACT

Microplastics in sediment cores from urban tidal tributaries, Barking and Bow Creek-London and salt marshes Swanscombe, Kent, and Rainham, Essex, Thames estuary (UK), were quantified by density separation and ATR-FTIR spectroscopy. All eight tributary cores were dominated by low-density microplastics, polypropylene, polyethylene, and polystyrene with the greatest abundance (mean 360.0 ± 12.0 particles 100 $g^{-1}$ dwt (0–10 cm depth) observed furthest from the confluence with the Thames due to storm tank combined-sewer-overflow input. Salt marsh core microplastics were highest at Swanscombe (mean 267.1 ± 10.2 particles 100 $g^{-1}$ dwt at 0–10 cm depth) in the high-marsh vegetation zone. Marsh sediment radionuclide dating ($Pb^{210}$, $Cs^{137}$) suggested a presence of microplastics in the sediment since at least the late 1950s, with increasing abundance towards surface sediments. Tidal tributaries and salt marshes of the Thames act as natural filters, with salt marshes accumulating microplastics over time and tributaries acting as both stores and sources depending on individual site conditions and hydrodynamic variability.

## 1. Introduction

Since achieving commercial success in the UK between the 1930s and 1960s, plastics have become increasingly commonplace in everyday situations (Thompson et al., 2009; BPF, 2014) (Fig. 1, Fig. S1). Plastics that are manufactured to be microscopic (primary) or have weathered to become microscopic (secondary) are known as microplastics (plastics >5 mm in size) (Barnes et al., 2009; Horton et al., 2017; GESAMP, 2019). Widespread environmental contamination by microplastic particles has been reported, although understanding of their behaviour, fate, and impact of ecological and human health is still being developed (Jambeck et al., 2015; Rochman, 2018; Bucci et al., 2020). Early reports of microplastics in the environment focused on marine accumulation, but as studies have expanded estuaries have been found to play a significant role in the microplastic source-fate-transport network (Sadri and Thompson, 2014; Jambeck et al., 2015). Estuaries link terrestrial sources to marine sinks and act as temporary stores by accumulating microplastics within their sediments (He et al., 2021; Ghinassi et al., 2023). Previous evaluations found microplastic abundance in river sediments were affected by a number of factors such as surrounding land use, seasonal variation, sewage outflows, and river geomorphology (Klein et al., 2015; Nel et al., 2018; Rodrigues et al., 2018; Lloret et al., 2021; Trusler et al., 2024). Within this, estuarine tributaries could also play a key role in the microplastic source-fate transport network and microplastic behaviour as they act both as concentrated sinks and as conduits for various other environmental pollutants (Babiarz et al., 2012; Vane et al., 2017; Lee and Shin, 2021).

There is a surprising dearth of microplastic abundance surveys within estuary salt marshes; these environments are ecologically valuable coastal buffers which are known to filter out and store other contaminants from the estuary, so they are likely to also play a key role in microplastic source-fate-transport pathways (Williams et al., 1994; Vane et al., 2020a, 2020b; Lloret et al., 2021). So far, salt marshes have been shown to net trap microplastics, with sequestration influenced by vegetation zone and flooding rate, indicating that certain marsh zones could be significant long-term stores of microplastics (Yao et al., 2019; Stead et al., 2020; Ogbuagu et al., 2022; Pinheiro et al., 2022). In addition, recent studies of sediment cores in estuaries and salt marshes have identified a possible link between microplastic sediment accumulation at depth and historical plastic consumption trends, as microplastic concentration decreased with depth (Willis et al., 2017; Li et al., 2020; Lloret et al., 2021). Based on this, it is conceivable that in certain

* Corresponding author.
*E-mail address:* chv@bgs.ac.uk (C.H. Vane).

https://doi.org/10.1016/j.marpolbul.2024.117360
Received 30 September 2024; Received in revised form 25 November 2024; Accepted 27 November 2024
Available online 3 December 2024

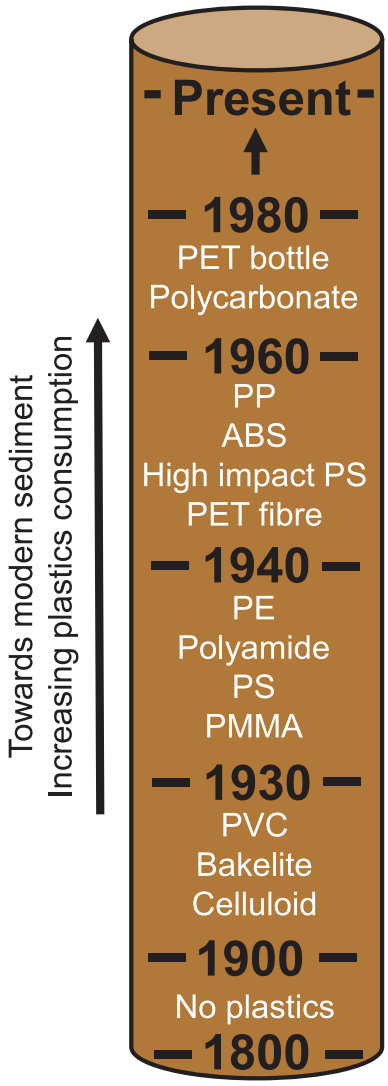


**Fig. 1.** Graphic of a dated sediment core showing when different microplastic typologies may first appear in the sediment record, based on an approximate timeline of UK plastics production and commercialisation (BPF, 2014; Plastics Europe, 2022). Note that there would be a consumption-waste-environment storage lag of unknown length that is not accounted for.

locations the sediment record contains a temporal record that combines plastics production and consumption trends as hypothesised in Fig. 1. Further investigation of this temporal-depth Anthropocene hypothesis alongside microplastic spatial variation is required to elucidate microplastic behaviour in these environments. This would be invaluable in establishing baselines and background microplastic concentrations and types within estuaries, relating historical environmental conditions, sources, and events to microplastic abundance trends through time as well as facilitating an understanding of the overall contaminant burden that spans chemicals (e.g. trace metals and organic compounds) and anthropogenic particles (e.g. microplastics and nanoparticles).

The Thames estuary (UK) is primarily an urban-industrial estuary which forms a major shipping transport route for the UK, including the London megacity built around it. The river has been of significant social and economic importance for the UK over hundreds of years and has had a long history of pollution. Its sediments have regularly been assessed for various chemical pollutants, including sewage compounds, trace metals, pharmaceuticals, polycyclic aromatic hydrocarbons (PAH), organochlorines, and brominated flame retardants (Scrimshaw and Lester, 1997; Murray et al., 2011; Pope et al., 2011; Vane et al., 2015; Ganci et al., 2019; Vane et al., 2020a; Vane et al., 2022; Downham et al., 2024). Recent studies have also found the Thames estuary to contain microplastics within both its sediments and water column, warranting further study to understand microplastic behaviour trends (Rowley et al., 2020; Devereux et al., 2023; Trusler et al., 2024).

In the present work, a sediment coring approach was employed in the estuary for the first time to evaluate how microplastic distribution and typology varied between two urban tributaries of the Thames estuary and two of its salt marshes. From this we sought to firstly identify hotspots of accumulation in tidal urban-industrial estuaries and highlight possible trends in microplastic behaviour, understanding how the vegetation, geomorphology, and hydrodynamic conditions of each environment impacted the microplastic record. In particular, the effect of elevation-distance and vegetation zone was explored for salt marshes, and the effect of distance from the confluence for two estuary tributaries was investigated. Cores were also used to explore the connection between microplastic abundance and sediment depth to understand whether sediments in tidal urban-industrial estuaries are long- or short-term stores of microplastics, and from this where the strongest temporal record of plastics consumption is likely to exist.

## 2. Methods

### 2.1. Study areas

The river Thames (UK) catchment spans an area of 14,000 km$^2$, generally flowing in an easterly direction from its source in Gloucestershire, before bisecting central London and discharging into the southern North Sea (Vane et al., 2022). The Thames becomes tidal below Teddington Weir in west London, spanning approximately 110 km of the river which are predominantly urban. All sites used in this study are connected to the tidal Thames estuary, either as tributaries or salt marshes.

Barking Creek (River Roding), London, is fully tidal below the Barking Barrage, generally flowing in a southerly direction through Barking before its confluence with the Thames on its north bank by the Barking Barrier and the outflow of Beckton Sewage Treatment Works (STW). Six samples were taken along a 2.65 km transect of Barking Creek starting from the Thames estuary confluence, known as UT1-UT6 (Fig. 2). Note that site UT4 was not analysed in this study. Bow Creek (River Lea), London, is a tidal meandering river below Bow Locks which bisects the London boroughs of Tower Hamlets and Newham. It discharges into the Thames on its north bank and is the most urban study area included in this study. Three core sites were sampled to give a transect of 0.78 km length starting from the Thames estuary conference, known as UT7-UT9 (Fig. 2). Specific locations and total core depth for each sampling site can be found in Table S1, while site images can be found in Fig. S2.

Swanscombe salt marsh (north Kent) is an urban marsh located on the Swanscombe Peninsula on the south bank of the Thames, and Rainham salt marsh is an urban marsh (south-west Essex) in Purfleet on the north bank (Fig. 2). Sampling transects of each marsh ran perpendicular to the flow of the Thames, with a sample taken from each vegetation zone which was in turn partly controlled by the elevational gradient relative to sea level. On Swanscombe salt marsh, the transect was 41.1 m long with samples TS1 (intertidal zone, no vegetation), TS2 and TS3 (low marsh, dominated by *Pelvetia canaliculata* and *Spartina* spp., respectively), TS4 and TS5 (high marsh, dominated by *Plantago maritima* and *Elytrigia atherica*, respectively). At Rainham salt marsh (Essex), a transect of 32.5 m consisted of TS6 (intertidal zone, no vegetation), TS7 (mid marsh, dominated by *Spartina* spp.), and TS8 (high marsh, dominated by *Elytrigia atherica*). Specific locations and total core depth for each sampling site can be found in Table S1, while site images can be found in Fig. S2.

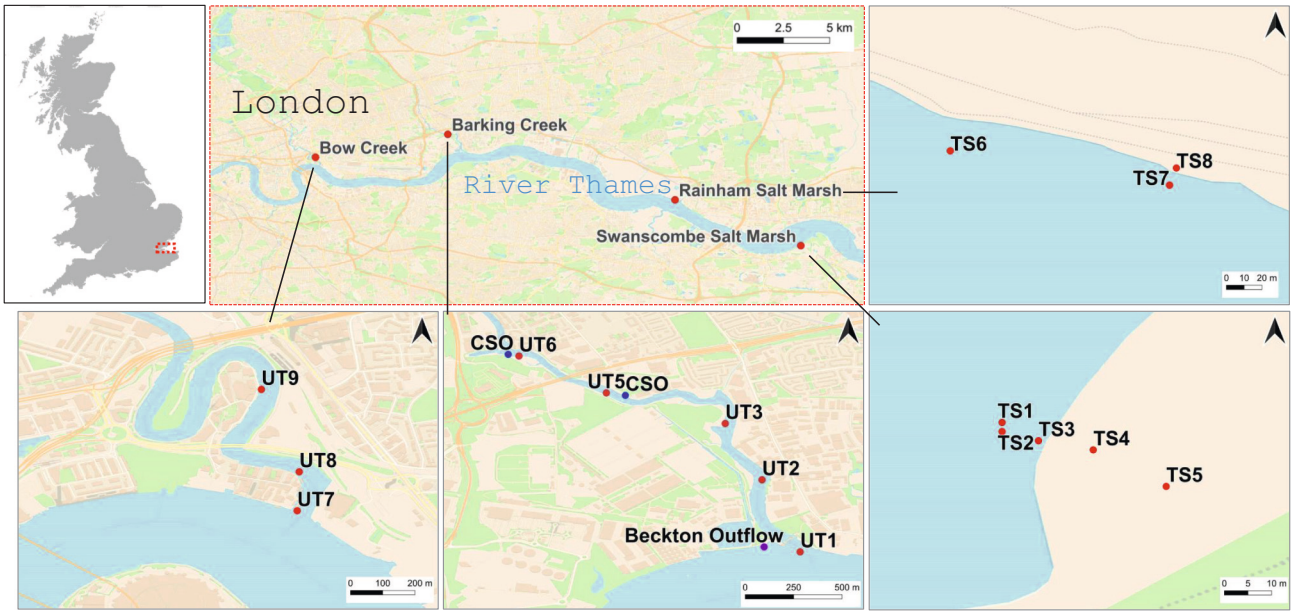


**Fig. 2.** Site map showing location of Thames estuary sediment core transects at Barking Creek (UT1–6), Bow Creek (UT7–9), Rainham salt marsh (TS1–5) and Swanscombe salt marsh (TS6–8), England, UK © OpenStreetMap contributors; Ordnance Survey data © Crown copyright and database right 2010–2023.

### 2.2. Sample collection and preparation

Estuary and tributary cores were obtained at low tide in February 2022 from a Port of London Authority Driftwood Dory tender (UT cores). For these samples, at each site a polycarbonate tube fitted with a stainless-steel basket catcher was driven into the exposed sediment to recover core material (as in Vane et al., 2007). The cores were contained in the tubes, capped and sealed for transportation to the laboratory in Nottingham (UK) and refrigerated upon arrival. The cores were then removed from the tubes by carefully pushing out the contents and sliced into 10 cm intervals so that downcore variation could be assessed. Samples were frozen for 24 h at −18 °C and freeze-dried using a freeze dryer (Alpha 1–4 LD, Martin Christ) at approximately 0.81 mbar and −55 °C.

Salt marsh cores (TS cores) were obtained at low tide on foot in June 2022 (images of each core can be found in Fig. S3). Depending on the local conditions at each sample site, either a polycarbonate tube fitted with a stainless-steel basket catcher was driven into the exposed sediment to recover core material (TS2, TS4, and TS5), or a Russian peat corer was used to extract three adjacent cores of 50 cm length (all other cores). In the case of the former technique, once extracted the cores were handled in the same way as for the UT cores. For those extracted with the Russian peat corer, three cores were required to generate sufficient sediment for replication in the lab (with an aim of obtaining 120 g of dry sediment per depth increment). In each instance, each of the three cores were sliced into 10 cm intervals in the field, and each interval was subsequently combined with the core material from the same 10 cm interval depths of the other cores from that site. This yielded a single composite sample for each sample site representing sediment depths 0–10 cm, 10–20 cm, 20–30 cm, 30–40 cm and 40–50 cm. These were then transported to the laboratory in Nottingham (UK) where they were frozen upon arrival at −18 °C. Samples were freeze-dried in the same way as the UT cores. Once dry, all samples from all sites were passed through a stainless steel Endecotts 5 mm sieve to obtain only the size fraction that would contain microplastic particles (<5 mm in size across its longest axis).

### 2.3. Chronology

Dried sediment samples from TS4, TS5, TS7 and TS8 cores were analysed for $^{210}$Pb, $^{226}$Ra, $^{137}$Cs and $^{241}$Am by direct gamma assay in the Environmental Radiometric Facility at University College London, using ORTEC HPGe GWL series well-type coaxial low background intrinsic germanium detector. Lead-210 was determined via its gamma emissions at 46.5 keV, and $^{226}$Ra by the 295 keV and 352 keV gamma rays emitted by its daughter isotope $^{214}$Pb following 3 weeks storage in sealed containers to allow radioactive equilibration. Cesium-137 and $^{241}$Am were measured by their emissions at 662 keV and 59.5 keV (Appleby et al., 1986). The absolute efficiencies of the detector were determined using calibrated sources and sediment samples of known activity. Corrections were made for the effect of self-absorption of low energy gamma rays within the sample (Appleby et al., 1992).

The chronologies presented for cores TS4, TS5, TS7 and TS8 were generated radiometrically from the Pb isotope ratio ($^{210}$Pb) and cesium ($^{137}$Cs) activity at each sediment depth interval to understand any age-depth relationships with the microplastic distribution (e.g. Vane et al., 2020a) using ORTEC HPGe GWL series well-type coaxial low background intrinsic germanium detector operated by the Environmental Radiometric Facility at University College London. It is noted that the coarse 10 cm sampling depth intervals used in this study mean that the dates conferred throughout are approximate.

### 2.4. Density separation and digestion

For each depth increment, 120 g dry sediment was analysed for microplastics via a density separation method, using four repetitions of 30 g dry sediment in order to generate an average microplastic abundance per 100 g dry sediment. In some cases, there was <120 g dry sediment left after the freeze-drying and sieving stages. These such samples were listed in Table S2 and have been noted in Figs. 4 and 5 using an asterisk (*).

The density separation method presented herein was developed from similar studies of microplastics in river sediments so that they would work most effectively for the clay- and organic- rich sediments specifically used in this study (Coppock et al., 2017; Horton et al., 2017; Tibbetts et al., 2018; Lloret et al., 2021). The method was tested for extraction efficiency using an intertidal sediment collected at Swanscombe marsh spiked with a known quantity of brightly coloured microplastics. A range of 8 plastic polymer types (x3 particles of each) of primary and secondary origin spanning densities between 0.9 and 1.58

g $cm^{-3}$ (polyethylene, polypropylene, polystyrene, PVC, PET, ABS, polyamide, and PMMA) were added to four repeats of 30 g sediment, ultimately obtaining an average recovery rate of 91.6 %.

In each case, 30 g dry sediment was added to a 600 ml glass beaker alongside a glass-coated magnetic stir bar, before 500 ml of zinc chloride ($ZnCl_2$) (at a density of 1.5 g $cm^{-3}$, filtered to 0.7 μm) was added. The sample was then stirred at 500 rpm on a magnetic stirrer (Fisherbrand™) for five minutes. Following this, the sample was left to settle for five minutes before quickly pulsing the sample at a high rpm three times to encourage air bubble removal. The sample was then topped up to within approximately a centimetre of the beaker's rim, before being covered with foil and left overnight to allow the sediments to settle at the bottom. The next morning, the sample was carefully (so as not to disturb the settled sediment) placed into a glass bowl, and additional $ZnCl_2$ was gently pipetted using a glass pipette down the interior side of the beaker to cause an overflow of $ZnCl_2$ and floating surface particles. A combination of gentle pouring and scooping with a metal spoon was then used to remove any remaining visible particles floating in the beaker, extracting a total of just under 150 ml of $ZnCl_2$. All exterior sides of the beaker were then rinsed three times with $ZnCl_2$ into the bowl to remove any particles adhered to them and the contents of the bowl subsequently washed into a 150 ml beaker. The sample was stirred briefly in the beaker, then covered with foil and left to settle for an hour. After this, the surface 100 ml was poured over a 10 μm polycarbonate filter under vacuum with a vacuum pump (KNF LABOPORT®), which was then rinsed with MilliQ ultrapure water under vacuum and placed into a 100 ml beaker for the next stage.

All $ZnCl_2$ was filtered under vacuum for reuse up to a maximum of seven times, filtering to 0.7 μm between each use to minimise contamination and maintain the density, as suggested in a previous study that found $ZnCl_2$ to retain 95 % efficiency after five reuses (Rodrigues et al., 2020). The density of each $ZnCl_2$ batch was checked after each use to ensure that the density of the $ZnCl_2$ remained consistently 1.5 g $cm^{-3}$ throughout its lifetime usage (Fig. S4).

Following density separation, samples underwent a 30 % hydrogen peroxide ($H_2O_2$) digest at 55 °C in a hot plate (Clifton™ HP1-3D, Nickel Electro™) with sand bath attachment for 72 h. For samples containing fewer organic particles (mostly UT samples), 25 ml of $H_2O_2$ was found to be sufficient to digest all organics, while TS samples which contained more organic matter required 40 ml of $H_2O_2$, and occasionally 48 h extra to ensure sufficient digestion of organic matter. Following digestion, samples were filtered under vacuum with a 10 μm polycarbonate filter, then rinsed three times using Milli-Q ultrapure water under vacuum to remove residual $H_2O_2$. The two filters (the filter placed into the beaker after the density separation, and the one used after the $H_2O_2$ digest) were then sealed in a petri dish within a box and left to air dry for seven days.

### 2.5. Identification and quantification

Once samples were dry, they were examined using a stereo microscope (SZX12, Olympus®) and external light source (KL1500, SCHOTT) at magnifications between 40× and 90×. Microplastic particles were identified using the criteria originally set out by Nor and Obbard (2014). Suspected microplastics had no cellular/organic structures visibly attached, were not shiny, and were of homogenous colour and texture. Adding to this, fibrous shapes of possible plastic origin were considered equally thick through their entire length (i.e. not segmented or tapered at the end) (Hidalgo-Ruz et al., 2012; Nor and Obbard, 2014). If a particle did not obviously conform to the above, it was examined under a higher magnification and tested for hardness via pressure using forceps (Hidalgo-Ruz et al., 2012; Tibbetts et al., 2018). Suspected microplastics were counted and sorted according to their shape and size: fragment, fibre, sphere, and large (1000–5000 μm) vs medium (10–1000 μm), respectively (small particles <10 um could not be analysed in this study). Particles were mounted on a glass slide for the sample, and sealed using another glass slide once examination was completed. Abundance was reported by average count per 100 g of dry weight sediment (particles 100 g $DW^{-1}$), with standard error of the mean (SEM) stated for calculated averages.

### 2.6. Chemical identification

Suspected microplastics from all depths of cores TS4, TS5, TS7, TS8, UT1 and UT7 were selected for analysis using Fourier-transform infrared (FTIR) spectroscopy. The TS cores were selected because they were the same cores that were radiometrically dated and the UT cores because they were at the confluences of their respective Thames tributaries. In each case, as many particles as reasonably scannable on at least one slide for the given depth increment were scanned using an FTIR (Cary 600 Series, Agilent Technologies) and an Attenuated Total Reflectance (ATR) module. Each particle on the slide was analysed between one and three times each, depending on the visible observed quality of the output spectrum. A total of 64 scans were used for each output, and 128 for a background scan which was ran frequently (approximately every hour) to reduce background noise in the outputs. The resolution was 4 $cm^{-1}$, using absorbance across spectrum wavelengths of 4000–950 $cm^{-1}$.

FTIR scans were processed to remove background noise and the $CO_2$ signal, then analysed using the Open Specy polymer matching software to match each particle scan to a material typology (Cowger et al., 2021). No preprocessing toggles were required, and the identification library used was the FTIR baseline corrected library. Successful matches to this database required a Pearson correlation score of over 0.7 to be accepted as positive identification. If this was not met, the particle was marked as 'unknown'. In such cases, it was likely that organic matter was adhered to the particle causing spectral interference, or that the particle had become significantly degraded and therefore not recognisable within the library database.

### 2.7. Contamination reduction and monitoring

Contamination could not be monitored during field collection stages, so all researchers wore fluorescent high visibility clothing which could be easily recognised during identification stages in the event of contamination. For samples collected in polycarbonate tubes, the tubes were thoroughly rinsed with de-ionised water before use, and collected sediments did not come in to contact with the air until they reached the laboratory for processing (aside from the very top and bottom of the cores which were promptly capped in the field). Petri dishes were left open on the lab bench during laboratory sample preparation to monitor any possible microplastic contamination of samples during this stage. A total of ±3 fibres possible contamination per whole depth increment was identified from these stages, with no fragments or spheres detected. Contamination was minimised during density separation and digestion steps by conducting these steps under a high flow fume hood, covering all equipment with foil when not in use, and rinsing all equipment with MilliQ water three times before immediate use. Researchers wore cotton laboratory coats and brightly coloured nitrile gloves during all laboratory stages, and where possible glass or metal equipment was used. To monitor possible contamination during these stages, at a randomly selected point during the life of a $ZnCl_2$ batch, a blank sample was processed whereby no sediment was added to the beaker at the start of the density separation stage, but was otherwise treated as normal though each subsequent stage. Contamination here averaged ±2 fibres per sample, no fragments or spheres were detected by any blank control. For fibres, the data reported herein should therefore be regarded with a possible total contamination of ±2–5 fibres.

## 3. Results

### 3.1. Thames urban tributary (UT) microplastic distribution

Microplastics were identified in all samples at all depth increments of UT cores. Microplastic concentrations within the sediments at all depth increments of the Barking Creek transect samples ranged from 55.8 ± 3.4 microplastic particles 100 g $DW^{-1}$ (UT1 0–10 cm depth) to 360.0 ± 12.0 particles 100 g $DW^{-1}$ (UT6 0–10 cm depth), with a mean of 126.6 particles 100 g $DW^{-1}$. Examination of surface 0–10 cm depths indicated the same abundance range, but with a higher mean of 156.7 particles 100 g $DW^{-1}$. Along the tributary transect, surface sediments were found to have a decreasing abundance with distance from UT6 towards UT1 at the Thames confluence (flow direction) (Fig. 3a). However, inspection of depth profiles indicated that this trend was not consistent across depth increments, offering different perspectives of microplastic abundance in these sediments (Fig. 4a-e). Cores UT3, UT5, and UT6 showed similar decreasing abundance with depth; UT1 and UT2 had more variable abundance. Sample UT5 (Barking Creek) was found to be contaminated at depth 30–40 cm by a polycarbonate swarf which had evaded preventative measures to remove them from the polycarbonate tubing that the sediments were collected in. Although easily identifiable, to prevent any of the contamination from potentially biasing the data, all microplastic abundance data at this depth was excluded from the dataset. This contamination was not found at any other depth increment or sample.

At the Bow Creek transect, the microplastic concentration across all depth increments had a smaller range from 50.0 ± 2.0 microplastic particles 100 g $DW^{-1}$ (UT9 0–10 cm depth) to 89.2 ± 6.5 particles 100 g $DW^{-1}$ (UT7 0–10 cm depth), with a mean of 72.6 particles 100 g $DW^{-1}$(Fig. 3b). Examination of surface 0–10 cm depths indicated the same abundance range, but with a slightly lower mean of 68.3 particles 100 g $DW^{-1}$. This transect was much shorter than the transect of Barking Creek with a smaller range, but data suggested a possible increasing abundance with distance from UT9 towards UT7 at the Thames confluence (seaward flow direction) (Fig. 3b). Investigation of the depth profiles revealed different trends for each core (Fig. 4f-h). To compare the abundance of microplastics in the surface 0–10 cm of sediments between Barking and Bow Creeks, the original individual repeat measurements for the transects were compared in a Mann-Whitney U non-parametric test, indicating a significant difference in microplastic abundance between the two rivers ($p = 0.01$, $W = 177.5$).

In terms of microplastic shape, spherical microplastics were in least abundance across both Barking and Bow Creek transects, with at least one depth increment in each core containing none. Across the Barking Creek transect, fragment shapes generally dominated core UT3, while fibres were more dominant at most depths in all other cores. In contrast at Bow Creek, fragments were consistently more abundant than fibres at all depth increments. In terms of size, medium microplastics (10 μm - 1000 μm in size) had decidedly greater abundance in comparison to large microplastics (1000 μm - 5000 μm) at all depths across both rivers (note that small microplastics <10 μm could not be analysed in the present study). FTIR scans of Thames confluence cores UT1 and UT7 indicated that 87.1 % and 90.4 % of suspected scanned microplastics could respectively be confirmed as of plastic origin, 12.9 % and 7.7 % as natural origin, and 0 % and 1.9 % could not be confidently identified (Fig. 5a, b). The most common plastics identified in UT1 were ranked (1) PET (22.6 %), (2) polypropylene, (3) polystyrene, and (4) polyethylene. In UT7, the most common were (1/2) polypropylene/polystyrene (19.2 % each), (3) polyamide, and (4) polyethylene. Distributions did not vary significantly downcore for each, with the four dominant types generally consistently so in all sediment layers.

### 3.2. Thames salt marsh (TS) microplastic distribution

Microplastics were detected in all depth increments of TS cores. Swanscombe marsh sediments at all depth increments contained microplastic abundances between the range of 4.4 ± 0.33 microplastic particles 100 g $DW^{-1}$ (TS5 60–70 cm depth) and 267.1 ± 10.2 particles 100 g $DW^{-1}$ (TS5 0–10 cm depth), with a mean of 101.4 particles 100 g $DW^{-1}$. Investigation of the surface 0–10 cm depth of all Swanscombe cores specified a range of 66.7 ± 3.5 particles 100 g $DW^{-1}$ (TS4) to 267.1 ± 10.2 particles 100 g $DW^{-1}$ (TS5), with a higher mean of 152.0

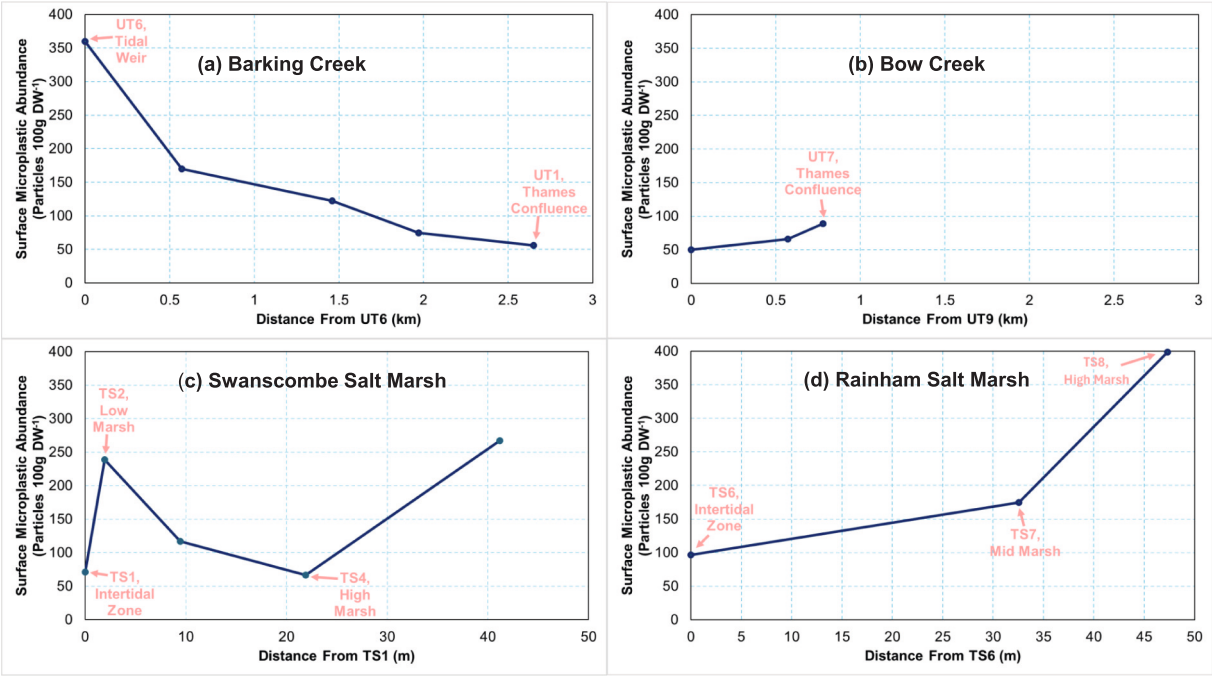


**Fig. 3.** Plot showing average surface sediment (0–10 cm) microplastic abundance with transect distance. Barking Creek, London, (b) Bow Creek, London, (c) Swanscombe salt marsh, Essex, (d) Rainham salt marsh, Kent, all sites along the river Thames estuary (UK). Note that distance is reported in kilometres for (a) and (b), and in metres for (c) and (d).

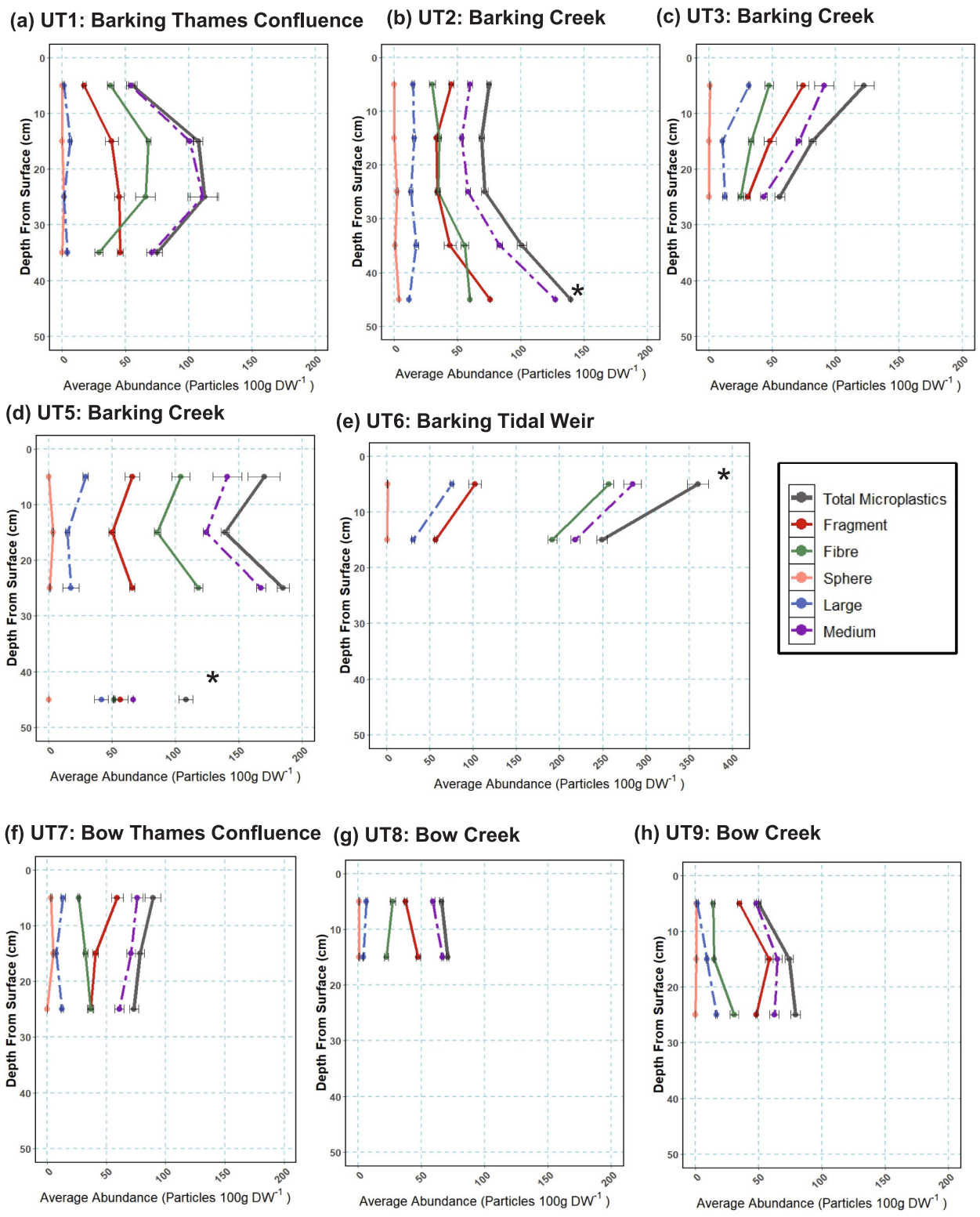


**Fig. 4.** Particle typology plots showing average concentrations of microplastics per 100 g sediment at each depth interval within the cores from each site along the transect of Barking Creek (a-e) and Bow Creek (f-h) (all London, UK). For each site, the total abundance is shown along with its constituent typology parts in terms of shape (fragment, fibres, and spheres) and size category (large 1000 μm −5000 μm microplastics and medium 10 μm- 1000 μm). Error bars denote the standard error of the mean. Samples marked with an asterisk (*) used less than the standard four repetitions due to lack of sediment following drying and sieving stages. Exact amounts presented in Table S2. Note that measurement at UT5 30–40 cm were excluded for the presence of contamination in the sample.

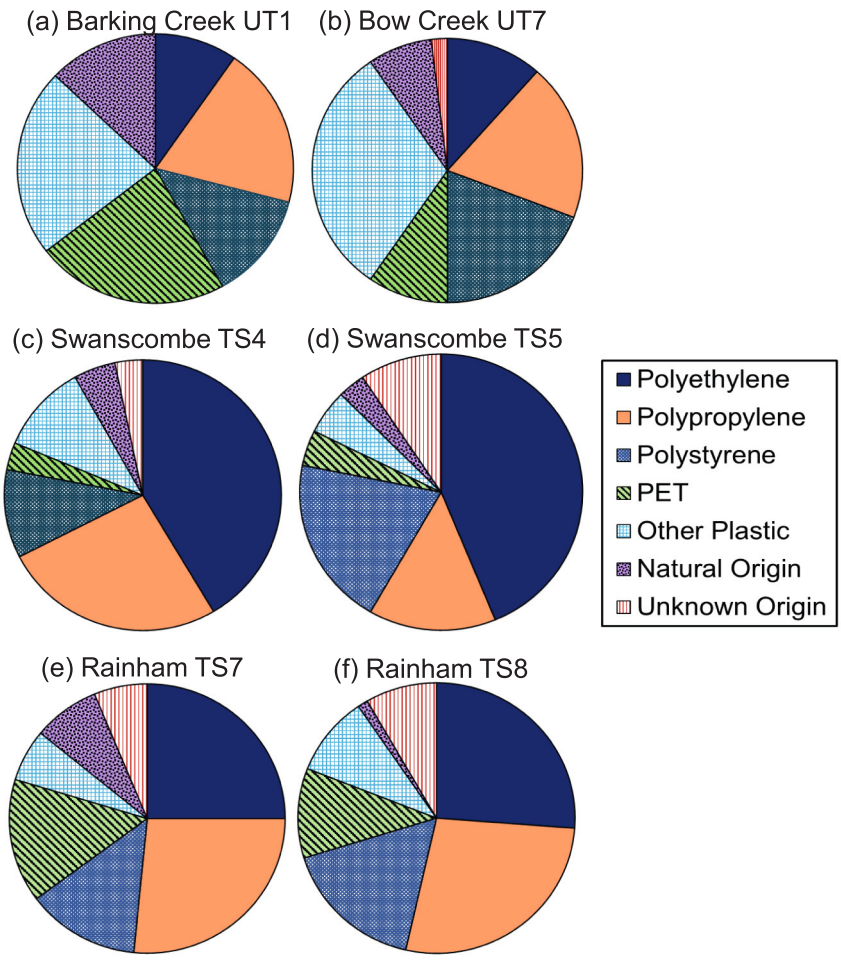


**Fig. 5.** Pie charts showing the material composition of suspected microplastics scanned using FTIR-ATR from the tributary and salt marsh cores: (a) Barking Creek, London, (b) Bow Creek, London, (c,d) Swanscombe salt marsh, Essex, and (e,f) Rainham salt marsh, Kent. Plastic types included under the 'other plastic' category included polyamide, acrylic, polycarbonate, polyurethane, ABS, and Polyvinyl chloride (PVC).

particles 100 g $DW^{-1}$. The abundance with distance along the transect away from TS1 (landward direction) for surface depths did not show a clear trend, with a spike in abundance at TS2 and TS5Exploration of the depth profiles for each Swanscombe core largely indicated a decreasing abundance of microplastics with depth, although this trend was clearer in some cores more than others (Fig. 6a-e). On the high marsh where the cores were radiometrically dated, core TS4 had a fluctuating abundance of microplastics which was lowest at the base and highest at 30–40 cm depth (possibly early 1960s). Radiometric dating indicated relatively high and changing sedimentation rates relating to irregular decline in $^{210}Pb$ activities in TS4. This could indicate anthropogenic disturbance to the sediment record or sedimentation processes which could have in turn influenced the microplastic accumulation rate. In contrast, TS5 abundance had more of an s-shaped profile with the lowest microplastic abundance of all samples recorded in the basal core. This then increased more rapidly from 30 to 40 cm (late 1960s) and then more slowly towards modern sediment.

Rainham marsh sediments contained microplastic abundances between 12.5 ± 0.75 particles 100 g $DW^{-1}$ (TS6 20–30 cm depth) and 398.9 ± 23.1 particles 100 g $DW^{-1}$ (TS8 0–10 cm depth), with a mean of 98.8 particles 100 g $DW^{-1}$. Investigation of the surface 0–10 cm depth of all Rainham cores ranged from 96.8 ± 4.3 particles 100 g $DW^{-1}$ (TS6) to 398.9 ± 23.1 particles 100 g $DW^{-1}$ (TS8), with a higher mean of 223.4 particles 100 g $DW^{-1}$. Along the transect, surface sediments were found to have an increasing abundance of microplastics with distance up the marsh from TS6 (Fig. 3d). Inspection of the depth profiles generally showed a decreasing abundance with distance from the surface sediment, although the specific trend was different for each core (Fig. 6f-h). For radiometrically dated core TS7, microplastic abundance significantly increased at 20–30 cm (1950s–1960s), and then remained largely consistent towards the surface depths. The chronology for TS8 indicated that sediments at 40–50 cm or deeper related to the 1960s, with a spike in abundance occurring at 20–30 cm towards modern sediment. To compare the abundance of microplastics in the surface 0–10 cm of sediments between Swanscombe and Rainham salt marshes, the original individual repeat measurements for the transects were compared in a Mann-Whitney U non-parametric test, indicating that there was no significant difference in microplastic abundance between the two salt marshes ($p = 0.24$, $W = 54.0$).

In terms of microplastic shape, spheres were the least abundant microplastic type across both salt marsh transects. Similarly, for both marshes, fibres were found to be the most dominant shape for low and mid marsh zones, while fragments dominated high marsh zones. In all cores, medium microplastics (10–1000 μm in size) had decidedly greater abundance in comparison to large microplastics (1000–5000 μm), except for at certain depths in cores TS5 (20–30 cm and 30–40 cm) and TS8 (0–10 cm) (note that small microplastics <10 μm could not be analysed in the present study). FTIR scans of dated cores TS4, TS5, TS7, and TS8 confirmed that respectively, 91.8 %, 87.5 %, 85.9 % and 90.5 % of suspected microplastics in each core were of certain plastic origin, generating an overall average of 88.8 %, with 4.7 % confirmed as natural origin and 6.5 % of unknown origin (Fig. 5c-f). Dominant plastic types were very similar for the two cores on each salt marsh, and also similar between the marshes. These were ranked for the whole of TS4

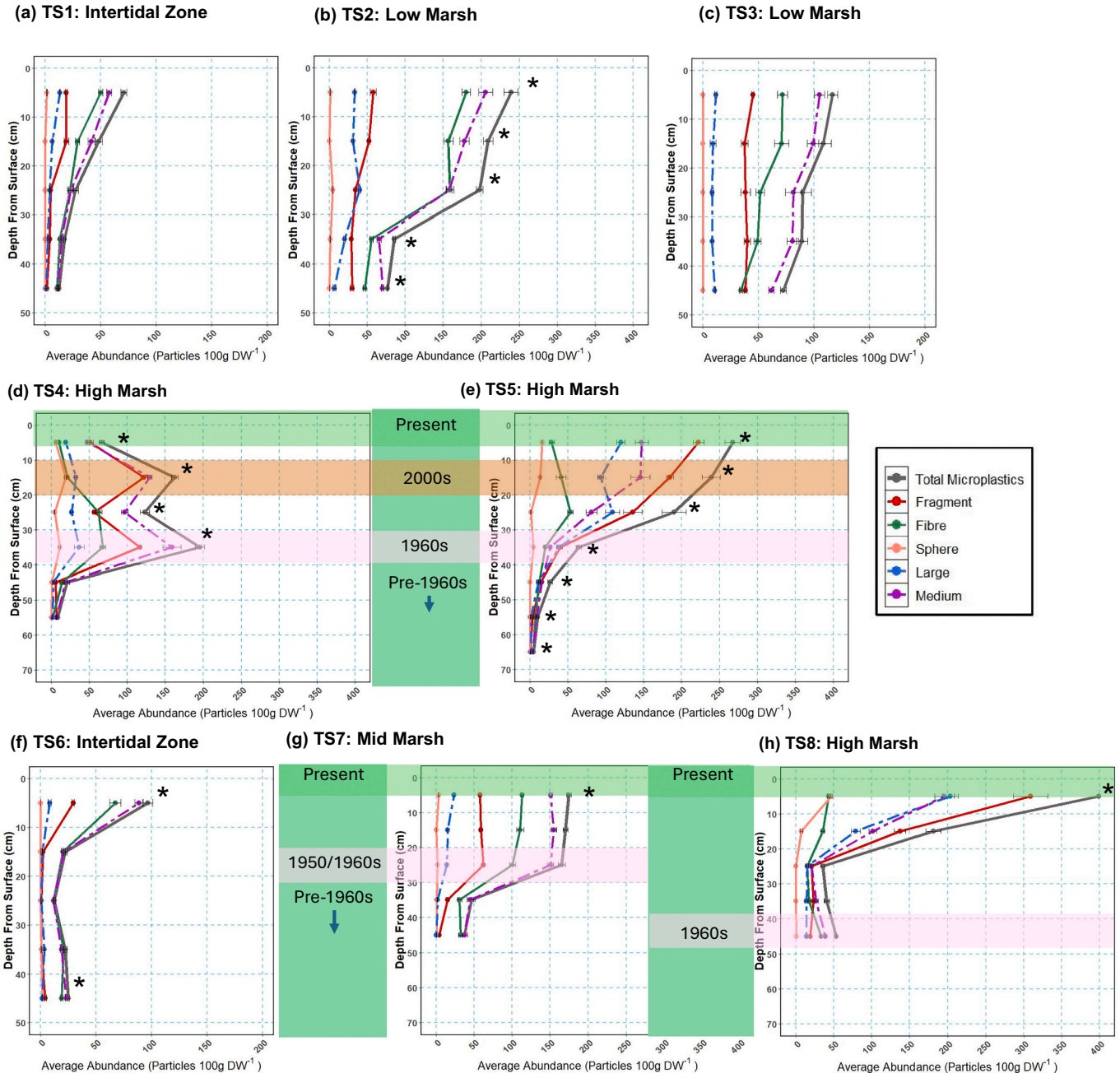


**Fig. 6.** Particle typology plots showing average concentrations of microplastics per 100 g sediment at each depth interval within the cores from each site along the transect of Swanscombe salt marsh (Kent, UK) (a-e) and Rainham salt marsh (Essex, UK) (f-h). For each site, the total abundance is shown along with its constituent typology parts in terms of shape (fragment, fibres, and spheres) and size category (large 1000 μm −5000 μm microplastics and medium 10–1000 μm). Error bars denote the standard error of the mean. For TS4 and TS5 the estimated chronology is provided, as based upon radiometric dating. Note that the coarse sampling intervals mean that the dates conferred are approximate. Samples marked with an asterisk (*) used less than the standard four repetitions due to lack of sediment following drying and sieving stages. Exact amounts presented in Table S2.

and TS5 cores (1) polyethylene (41.5 % and 43.8 %, respectively), (2) polypropylene, (3) polystyrene, and (4) PET at Swanscombe, and for TS7 and TS8 (1) polypropylene (26.6 % and 27.4 %, respectively), (2) closely polyethylene, and (3/4) polystyrene/PET at Rainham. Distributions did not vary significantly downcore, with the four dominant types generally consistently so in all sediment layers.

## 4. Discussion

All samples used in the study were found to contain microplastics. Microplastic abundances were generally greatest within the high salt marsh vegetation zone and lowest in the tributaries. Sediments from Bow Creek contained some of the lowest microplastic concentrations in the study, with average abundances that were significantly different to the abundance at Barking Creek. This short Bow Creek transect was also dominated by fragment shapes, while Barking Creek microplastics were primarily fibres. Microplastic fibres largely originate from the laundering of fabrics which then enter the sewage network and can ultimately be discharged into waterways at point source outflows (Browne et al., 2011; Zambrano et al., 2019; Frost et al., 2022). There were no such known point sources of microplastics entering Bow Creek in the transect vicinity but there were across the Barking Creek transect (one

each in proximity to UT1 and UT6, plus one between UT3 and UT5), which may in part explain the difference in abundance of microplastics and plastic morphology dominance at these sites. In addition, sites on Barking Creek are proximately protected by the Barking Barrier during storm surges while Bow Creek is more indirectly protected by the Thames Barrier that it is situated upstream of. During dynamic high flows microplastics can be flushed out from surface sediments, so it may be logical that under storm surge conditions microplastics are more readily flushed from the Bow Creek sediments into the estuary in comparison to Barking Creek due to the proximity of the barrier (Hurley et al., 2018; Ockelford et al., 2020; Pinheiro et al., 2022). This would indicate that flood management practices influence the microplastic trapping ability of tributary sediments.

Investigation of the point source outflows along the Barking Creek transect highlighted site UT6, as the sediment here contained a considerably higher abundance than all other tributary cores. This site was the closest downstream site to a combined sewer overflow CSO (Folkestone Road pumping station storm tanks) (<40 m upstream) which may have contributed to the high microplastic fibre load. UT6 was also located immediately downstream of the Barking Barrage (tidal boundary) on the outside bend of a meander and also by the discharge point of Hand Trough Creek. These local conditions are likely to generate complex flows with changing water density at this site, all of which may encourage the deposition of microplastics within the sediment. This observation aligns with previous reports indicating high microplastic loads in sediments and surface waters by CSO outflow courses, giving further credence to the notion that CSOs are major microplastic sources for rivers, and that their outflows are hotspots of accumulation (Dris et al., 2018; Polanco et al., 2020; Rowley et al., 2020; Trusler et al., 2024). The effect of CSO outflows on microplastic concentration should therefore be considered in future monitoring and management programmes.

In contrast, site UT1 near to Beckton STW did not show signs of an elevated microplastic concentration despite a dominance of fibres in the sediment, in agreement with an earlier study of Thames estuary surface sediments at the Beckton outflow in 2020 (Trusler et al., 2024). Based on this, it could be argued that Beckton STW treatment processes were effective at removing microplastics from wastewater; STWs have previously been found to remove between 83 % and 99 % of microplastic contamination from wastewater (Murphy et al., 2016; Dris et al., 2018; Kay et al., 2018). However, a previous study of the surface waters close to Beckton STW did record high concentrations of microplastics in the water column, as have studies of both sediments and surface waters near to other UK STWs (Horton et al., 2017; Kay et al., 2018; Woodward et al., 2021; Devereux et al., 2023). As suggested in Trusler et al., 2024, it could therefore alternatively be that the tidal Thames estuary causes sufficient flow turbulence such that microplastics are not stored locally in the sediment at Beckton but are dispersed further downstream via the water column, resulting in a comparatively low abundance of microplastics within sediments in proximity to the outflow. STWs cannot therefore be overlooked as microplastic conduits and should be considered alongside other human activities such as CSO outflows and flood management when selecting sites for microplastic assessment and monitoring as these factors are all likely to have significant influence on microplastic distribution and behaviour.

Downcore abundances for each tributary core showed different trends - while some exhibited the anticipated decreasing abundance of microplastics with depth, others showed the opposite, and some suggested no trend at all. A lack of a consistent downcore trend in the tributary sediments may reflect the dynamic tidal nature of these tributaries whereby their complex flows cause the flushing of microplastics from some of the sites and accumulation at others (Hurley et al., 2018; Ockelford et al., 2020; Pinheiro et al., 2022). Other factors such as bioturbation that affect sediment accumulation and scour rate could also impact o microplastics distribution and should be investigated further (Pinheiro et al., 2022). These complex conditions may mean that tidal urban-industrial tributary sediments are not consistently long-term stores of microplastics, rather they act as both stores and sources depending on site conditions and hydrodynamic variability.

All samples across the tributaries and salt marshes had a similar overall composition of microplastic types. This composition was closely related to the most commonly manufactured types of plastic, in agreement with several other studies of microplastics in river sediments and salt marshes compositions (Matsuguma et al., 2017; Fan et al., 2019; Yao et al., 2019; Li et al., 2020; Plastics Europe, 2022; Pinheiro et al., 2022; Trusler et al., 2024). This could suggest that the sediment microplastic abundance is a good reflection of plastics in circulation. Additionally, the dominant low-density plastic types (e.g. polyethylene and polypropylene) are naturally buoyant in most estuaries, giving them a higher transport mobility than other microplastic types (He et al., 2021). It is also important to note that the density-based separation method followed in this study and similar reports is likely to be somewhat bias towards lower density polymers, and therefore the abundance of higher density microplastics (>1.5 g $cm^{-3}$) will be underrepresented.

Both Swanscombe and Rainham salt marsh sediments contained microplastic abundances that were not significantly different from one another despite geographic and hydrodynamic differences, implying the behaviour of microplastics in these environments is similar. The two marshes also generally showed that surface microplastic abundance was not homogenous and increased with elevation-distance from low to high marsh vegetation zones, in agreement with a previous case study of a Brazilian salt marsh (Pinheiro et al., 2022). Natural increases in elevation-distance within a salt marsh is well known to reduce the flow velocity so that lower marsh zones regularly interact with the estuary and attenuate wave energy as it travels up the marsh (Adam, 1990; Schoutens et al., 2019). As this wave energy is attenuated, it is logical that any microplastics transported within the flow from the estuary are deposited due to the loss of energy, therefore leading to a higher concentration of microplastics higher up the marsh in comparison to the intertidal zone. In addition, the presence of marsh vegetation (which in turn is partly controlled by elevation-distance) has previously been found to specifically encourage the trapping of microplastics within salt marshes by altering flow turbulence and shear stress even under high flow conditions in comparison to bare intertidal zones (Yao et al., 2019; Ogbuagu et al., 2022). This would make both the estuary a major source of microplastics for a tidal salt marsh, and the marsh a significant store for the estuary, corroborating a previous study that identified a net trapping of microplastics on another UK salt marsh (Stead et al., 2020). This is also mirrored by the similar composition of microplastics across both the tributaries and salt marshes as it indicates that the salt marsh plastics are from the same sources are those deposited in the tributaries.

The lower abundance of microplastics in the low marsh zone could be attributed to its more frequent interaction with the estuary and low biomass. This means that these zones (especially intertidal sites TS1 and TS6) behave more similarly to the tributary sites and contain more similar concentrations of microplastics. Site TS2 was highlighted as a low marsh accumulation hotspot, which could be attributable to its unique sampling location on the salt marsh wrack line and first vegetated marsh zone. This suggests that microplastics are routinely deposited on the wrack line as the normal high tide recedes. High microplastic accumulation at both study site high marshes could then relate to microplastic deposition during higher flows and storm surges. During these conditions, the microplastic load of the estuary is likely to be higher than is typical (Hurley et al., 2018; Ockelford et al., 2020; Pinheiro et al., 2022) and the flow is driven further up the marsh, where denser vegetation results in high marsh storm deposits that contain higher concentrations of microplastics than the lower marsh. As a result, the high marsh zone sediments may give indications of estuary peak microplastic loads which could be important for regular microplastic monitoring studies. Radiometric dating was therefore carried out for high marsh cores TS4, TS5, TS7, and TS8 to identify whether there was a temporal record of microplastics contained within the sediment.

Inspection of downcore microplastic profiles revealed all cores except for TS4 had a decline in abundance with depth (albeit to different specific extents for each). This agrees with past studies of salt marsh sediment cores which proposed a temporal link between microplastic abundance and salt march sediment depth (Li et al., 2020; Lloret et al., 2021). Microplastic records for all dated cores confirmed either low or a marked decrease in microplastic abundance before the 1960s, a period when plastics began to achieve widespread commercial significance and before marine plastic debris was first recorded in the 1970s (Carpenter et al., 1972; Carpenter and Smith, 1972; Thompson et al., 2009). The consistent radiometric profiles for all cores except for TS4 confirms that the vertical remobilisation of the microplastics at these sites can be ruled out (Simon-Sánchez et al., 2022). This is also consistent with other studies who reported low or nil microplastic concentrations in sediments around the mid-20th century (Matsuguma et al., 2017; Willis et al., 2017; Lloret et al., 2021; Simon-Sánchez et al., 2022). In 1950, Global plastics production was around 1.5 Mt., and their production has continued to rise over time, reaching over 200 Mt. in 2000, up to 380 Mt. in 2015 (Plastics Europe, 2006; Geyer et al., 2017). In agreement, the low basal core abundance increased towards modern sediments, suggesting that as UK plastic consumption increased, as did the abundance of microplastics in the salt marsh sediment record. These salt marshes are therefore long-term stores of microplastics and showcase a marked presence of plastics-related anthropogenic activity within Thames estuary since at least the 1960s.

No core was found to reach a pristine zero abundance at its base, although the base of TS5 (pre 1960s) contained only fibrous microplastics that were within the fibre contamination error established *in this* study (4.4 ± 0.33 microplastic particles 100 $g^{-1}$ in TS5, 60–70 cm depth). Consequently, it is not possible to ascertain whether the few microplastics fibres were wholly derived from procedural contamination or represent a low abundance combination of sources including microplastics that are contemporary with sediment interval (e.g. pre 1960s).

## 5. Conclusion

This study has revealed for the first time the accumulation of microplastics in Thames estuary tributary and salt marsh sediments through the analysis of sediment cores. On the Thames estuary tributaries, Bow Creek sediments on average contained lower concentrations of microplastics than those of Barking Creek, and inferences could be made as to microplastic behaviours that led to variable surface abundance between tributaries as well as individual sites. Downcore variations were also variable, indicating that tributary sediments may act both as stores and sources of microplastics within the Thames estuary depending on specific conditions such as geomorphology, human interventions, and hydrodynamics. Analysis beyond surface microplastic distributions is therefore important for providing additional site information and data about microplastic behaviour which could aid in building a more holistic depiction of microplastic source-fate-transport mechanisms and spatiotemporal variation.

Salt marsh microplastic accumulation increased with distance up the marsh, which was suggested to be controlled at least in part by natural changes in elevation-distance and vegetation between marsh zones. Sites situated along the wrack line should also be considered when selecting marsh sampling sites as it may cause under/overestimations of microplastic concentrations for lower marsh zones. Vegetated sites higher up the marsh were identified as long-term stores of microplastics, generally showing increased microplastic abundance from basal cores towards modern sediments. This is likely to reflect changes in plastics consumption through time, meaning that as plastics consumption increased in the UK since the mid-20th century, as did the accumulation of microplastics in salt marsh sediments. Salt marshes are therefore important components of microplastic source-fate-transport networks. Sites at the back of the marshes contained some of the most undisturbed microplastic records, with dated cores containing records from just before the 1960s when widespread plastics consumption began in the UK. These cores may also contain storm deposits and therefore reflect some of the peak microplastic transportation periods across the estuary, making high marshes valuable sites for future sampling in similar tidal urban-industrial estuaries and further developing understanding of the microplastic source-fate-transport mechanisms within them.

## CRediT authorship contribution statement

**Megan M. Trusler:** Writing – original draft. **Sarah Cook:** Supervision. **Barry H. Lomax:** Supervision. **Christopher H. Vane:** Writing – review & editing, Conceptualization.

## Declaration of competing interest

The authors declare that they have no known competing financial interests or personal relationships that could have appeared to influence the work reported in this paper.

## Acknowledgement

Support for Megan Trusler PhD studentship was provided by the University of Nottingham. Core collection was funded by British Geological Survey (BGS), Organic Geochemistry Facility (NEE4699S). The Port of London Authority is thanked for their assistance in accessing sites at Barking and Bow Creek. The University College London Environmental Radiometric Facility (Dr Hangdong Yang) is thanked for dating sediment sequences and Royal Society for the Protection of Birds (Jamie Smith) is thanked for faciliting access to Rainham salt marsh. This paper is published with the permission of the Executive Director, BGS.

## Appendix A. Supplementary data

Supplementary data to this article can be found online at https://doi.org/10.1016/j.marpolbul.2024.117360.

## Data availability

Data will be made available on request.

## References

Adam, P., 1990. 1- General Features of Saltmarshes and Their Environment. In: Saltmarsh Ecology. Cambridge University Press, Cambridge, UK, pp. 1–70.

Appleby, P.G., Nolan, P.J., Gifford, D.W., Godfrey, M.J., Oldfield, F., Anderson, N.J., Battarbee, R.W., 1986. $^{210}$Pb dating by low background gamma counting. Hydrobiologia 143, 21–27.

Appleby, P.G., Richardson, N., Nolan, P.J., 1992. Self-absorption corrections for well-type germanium detectors. Nuclear Instruments & Methods in Physics Research Section B-Beam Interactions with Materials and Atoms 71 (2), 228–233.

Babiarz, C., Hoffmann, S., Wieben, A., Hurley, J., Andren, A., Shafer, M., Armstrong, D., 2012. Watershed and discharge influences on the phase distribution and tributary loading of total mercury and methylmercury into Lake Superior. Environ. Pollut. 161, 299–310. https://doi.org/10.1016/j.envpol.2011.09.026.

Barnes, D.K.A., Galgani, F., Thompson, R.C., Barlaz, M., 2009. Accumulation and fragmentation of plastic debris in global environments. Philos. Trans. R. Soc. B 364 (1526), 1985–1998. https://doi.org/10.1098/rstb.2008.0205.

British Plastics Federation, 2014. A History of Plastics [Online]. Available at: https://www.bpf.co.uk/plastipedia/plastics_history/Default.aspx [Accessed: 25/07/2024].

Browne, M.A., Crump, P., Niven, S.J., Teuten, E., Tonkin, A., Galloway, T., Thompson, R., 2011. Accumulation of microplastic on shorelines woldwide: sources and sinks. Environ. Sci. Technol. 45 (21), 9175–9179. https://doi.org/10.1021/es201811s.

Bucci, K., Tulio, M., Rochman, C.M., 2020. What is known and unknown about the effects of plastic pollution: a meta-analysis and systematic review. Ecol. Appl. 30 (2), e02044. https://doi.org/10.1002/eap.2044.

Carpenter, E.J., Smith, K.L., 1972. Plastics on the Sargasso Sea surface. Science 175 (4027), 1240–1241. https://doi.org/10.1126/science.175.4027.1240.

Carpenter, E.J., Anderson, S.J., Harvey, G.R., Miklas, H.P., Peck, B.B., 1972. Polystyrene spherules in coastal waters. Science 178 (4062), 749–750. https://doi.org/10.1126/science.178.4062.749.

Coppock, R.L., Cole, M., Lindeque, P.K., Queirós, A.M., Galloway, T.S., 2017. A small-scale, portable method for extracting microplastics from marine sediments. Env. Pollut. 230, 829–837. https://doi.org/10.1016/j.envpol.2017.07.017.
Cowger, W., Steinmetz, Z., Gray, A., Munno, K., Lynch, J., Hapich, H., Primpke, S., Frond, H.D., Rochman, C., Herodotou, O., 2021. Microplastic spectral classification needs an open source community: open specy to the rescue. Anal. Chem. 93, 7543–7548. https://doi.org/10.1021/acs.analchem.1c00123.
Devereux, R., Ayati, B., Westhead, E.K., Jayaratne, R., Newport, D., 2023. The great source microplastic abundance and characteristics along the river Thames. Mar. Pollut. Bull. 191, 114965. https://doi.org/10.1016/j.marpolbul.2023.114965.
Downham, R.P., Gannon, B., Lozano, D.C.P., Jones, H.E., Vane, C.H., Barrow, M.P., 2024. Tracking the history of polycyclic aromatic compounds in London through a River Thames sediment core and ultrahigh resolution mass spectrometry. J. Hazard. Mater. 473, 134605. https://doi.org/10.1016/j.jhazmat.2024.134605.
Dris, R., Gasperi, J., Tassin, B., 2018. Sources and fate of microplastics in urban areas: A focus on Paris megacity. In: Wagner, M., Lambert, S. (Eds.), The Handbook of Environmental Chemistry (58): Freshwater Microplastics: Emerging Environmental Contaminants? Springer International Publishing AG, Cham, Switzerland, pp. 69–83.
Fan, Y., Zheng, K., Zhu, Z., Chen, G., Peng, X., 2019. Distribution, sedimentary record, and persistence of microplastics in the Pearl River catchment, China. Environ. Pollut. 251, 862–870. https://doi.org/10.1016/j.envpol.2019.05.056.
Frost, H., Bond, T., Sizmur, T., Felipe-Sotelo, M., 2022. A review of microplastic fibres: generation, transport, and vectors for metal(loid)s in terrestrial environments. Environ. Sci: Processes & Impacts 24, 504–524. https://doi.org/10.1039/D1EM00541C.
Ganci, A.P., Vane, C.H., Abdallah, M.A.-E., Moehring, T., Harrad, S., 2019. Legacy PBDEs and NBFRs in sediments of the tidal river Thames using liquid chromatography coupled to a high resolution accurate mass orbitrap mass spectrometer. Sci. Total Environ. 658, 1355–1366. https://doi.org/10.1016/j.scitotenv.2018.12.268.
Geyer, R., Jambeck, J.R., Law, K.K., 2017. Production, use, and fate of all plastics ever made. Sci. Adv. https://doi.org/10.1126/sciadv.1700782.
Ghinassi, M., Michielotto, A., Uguagliati, F., Zattin, M., 2023. Mechanisms of microplastics trapping in river sediments: insights from the Arno River (Tuscany, Italy). Sci. Total Environ. 866, 161273. https://doi.org/10.1016/j.scitotenv.2022.161273.
Group of Experts on the Scientific Aspects of Environmental Protection (GESAMP), 2019. In: Kershaw, P., Turra, A., Galgani, F. (Eds.), Guidelines for the Monitoring and Assessment of Plastic Litter in the Ocean. United Nations Office Nairobi (UNON), Publishing Services Section: Group of Experts on the Scientific Aspects of Environmental Protection (GESAMP).
He, B., Smith, M., Egodawatta, P., Ayoko, G.A., Rintoul, L., Goonetilleke, A., 2021. Dispersal and transport of microplastics in river sediments. Environ. Pollut. 279, 116884. https://doi.org/10.1016/j.envpol.2021.116884.
Hidalgo-Ruz, V., Gutow, L., Thompson, R.C., Thiel, M., 2012. Microplastics in the marine environment: a review of the methods used for identification and quantification. Environ. Sci. Technol. 46 (6), 3060–3075. https://doi.org/10.1021/es2031505.
Horton, A.A., Svendsen, C., Williams, R.J., Spurgeon, D.J., Lahive, E., 2017. Large microplastic particles in sediments of tributaries of the river Thames, UK – abundance, sources and methods for effective quantification. Mar. Pollut. Bull. 114 (1), 218–226. https://doi.org/10.1016/j.marpolbul.2016.09.004.
Hurley, R.R., Woodward, J., Rothwell, J.J., 2018. Microplastic contamination of river beds significantly reduced by catchment-wide flooding. Nat. Geosci. 11 (4), 251–257. https://doi.org/10.1038/s41561-018-0080-1.
Jambeck, J.R., Geyer, R., Wilcox, C., Siegler, T.R., Perryman, M., Andrady, A., Narayan, R., Law, K.L., 2015. Plastic waste inputs from land into the ocean. Science 347 (6223), 768–771. https://doi.org/10.1126/science.1260352.
Kay, P., Hiscoe, R., Moberley, I., Bajic, L., Mckenna, N., 2018. Wastewater treatment plants as a source of microplastics in river catchments. Env. Sci. Pol. 25 (20), 20264–20267. https://doi.org/10.1007/s11356-018-2070-7.
Klein, S., Worch, E., Knepper, T.P., 2015. Occurrence and spatial distribution of microplastics in river shore sediments of the Rhine-Main area in Germany. Environ. Sci. Technol. 49 (10), 6070–6076. https://doi.org/10.1021/acs.est.5b00492.
Lee, H.-S., Shin, H.-S., 2021. Evaluation of pollutants characteristics and effect of dissolved and particulate contaminants in tributaries of an urban watershed. Sci. Tot. Env. 785, 147259. https://doi.org/10.1016/j.scitotenv.2021.147259.
Li, J., Huang, W., Xu, Y., Jin, A., Zhang, D., Zhang, C., 2020. Microplastics in sediment cores as indicators of temporal trends in microplastic pollution in Andong salt marsh, Hangzhou Bay, China. Regional Studies in Marine Science 35, 101149. https://doi.org/10.1016/j.rsma.2020.101149.
Lloret, J., Pedrosa-Pamies, R., Vandal, N., Rorty, R., Ritchie, M., Mcguire, C., Chenoweth, K., Valiela, I., 2021. Salt marsh sediments act as sinks for microplastics and reveal effects of current and historical land use changes. Environ Adv. 4, 100060. https://doi.org/10.1016/j.envadv.2021.100060.
Matsuguma, Y., Takada, H., Kumata, H., Kanke, H., Sakurai, S., Suzuki, T., Itoh, M., Okazaki, Y., Boonyatumanond, R., Zakaria, M.P., Weerts, S., Newman, B., 2017. Microplastics in sediment cores from Asia and Africa as indicators of temporal trends in plastic pollution. Arch. Environ. Contam. Toxicol. 73 (2), 230–239. https://doi.org/10.1007/s00244-017-0414-9.
Murphy, F., Ewins, C., Carbonnier, F., Quinn, B., 2016. Wastewater treatment works (Wwtw) as a source of microplastics in the aquatic environment. Environ. Sci. Technol. 50 (11), 5800–5808. https://doi.org/10.1021/acs.est.5b05416.
Murray, D., Dempsey, P., Lloyd, P., Murray, D., Dempsey, P., Lloyd, P., 2011. Copper in the Thames estuary in relation to the special protection areas. Hydrobiologia 672 (1), 39–47. https://doi.org/10.1007/s10750-011-0756-7.
Nel, H.A., Dalu, T., Wasserman, R.J., 2018. Sinks and sources: assessing microplastic abundance in river sediment and deposit feeders in an austral temperate urban river system. Sci. Total Environ. 612, 950–956. https://doi.org/10.1016/j.scitotenv.2017.08.298.
Nor, N.H.M., Obbard, J.P., 2014. Microplastics in Singapore's coastal mangrove ecosystems'. Mar. Pollut. Bull. 79 (1–2), 278–283. https://doi.org/10.1016/j.marpolbul.2013.11.025.
Ockelford, A., Cundy, A., Ebdon, J.E., 2020. Storm response of fluvial sedimentary microplastics. Scientific Reports 10 (1), 1865. https://doi.org/10.1038/s41598-020-58765-2.
Ogbuagu, C.C., Kassem, H., Udiba, U.U., Stead, J.L., Cundy, A.B., 2022. Role of saltmarsh systems in estuarine trapping of microplastics. Sci. Rep. 12 (1), 15546. https://doi.org/10.1038/s41598-022-18881-7.
Pinheiro, L.M., Britz, L.M.K., Agostini, V.O., Pérez-Parada, A., García-Rodríguez, F., Galloway, T.S., Pinho, G.L.L., 2022. Salt marshes as the final watershed fate for meso- and microplastic contamination: a case study from southern Brazil. Sci. Total Environ. 838 (2), 156077. https://doi.org/10.1016/j.scitotenv.2022.156077.
Plastics Europe, 2006. The Compelling Facts About Plastics: An Analysis of Plastic Production, Demand and Recovery for 2006 in Europe [Online]. Available at: https://plasticseurope.org/wp-content/uploads/2021/10/2006-Compelling-facts.pdf [Accessed: 20/11/2024].
Plastics Europe, 2022. Plastics-the Facts 2022 [Online]. Available at: https://plasticseurope.org/knowledge-hub/plastics-the-facts-2022/ [Accessed: 10/06/2024].
Polanco, H., Hayes, S., Roble, C., Krupitsky, M., Branco, B., 2020. The presence and significance of microplastics in surface water in the lower Hudson River estuary 2016–2019: a research note. Mar. Pollut. Bull. 161, 111702. https://doi.org/10.1016/j.marpolbul.2020.111702.
Pope, N.D., Langston, W.J., Pope, N.D., Langston, W.J., 2011. Sources, distribution and temporal variability of trace metals in the Thames estuary. Hydrobiologia 672 (1), 49–68. https://doi.org/10.1007/s10750-011-0758-5.
Rochman, C.M., 2018. Microplastics research—from sink to source. Science 360 (6384), 28–29. https://doi.org/10.1126/science.aar7734.
Rodrigues, M.O., Abrantes, N., Gonçalves, F.J.M., Nogueira, H., Marques, J.C., Gonçalves, A.M.M., 2018. Spatial and temporal distribution of microplastics in water and sediments of a freshwater system (Antuã River, Portugal). Sci. Total Environ. 633, 1549–1559. https://doi.org/10.1016/j.scitotenv.2018.03.233.
Rodrigues, M.O., Gonçalves, A.M.M., Gonçalves, F.J.M., Abrantes, N., 2020. Improving cost-efficiency for MPS density separation by zinc chloride reuse. MethodsX 7, 100785. https://doi.org/10.1016/j.mex.2020.100785.
Rowley, K.H., Cucknell, A.-C., Smith, B.D., Clark, P.F., Morritt, D., 2020. London's river of plastic: high levels of microplastics in the Thames water column. Sci. Total Environ. 740, 140018. https://doi.org/10.1016/j.scitotenv.2020.140018.
Sadri, S.S., Thompson, R.C., 2014. On the quantity and composition of floating plastic debris entering and leaving the Tamar estuary, Southwest England. Mar. Pollut. Bull. 81 (1), 55–60. https://doi.org/10.1016/j.marpolbul.2014.02.020.
Schoutens, K., Heunrt, M., Minden, V., Schulte Ostermann, T., Silinski, A., Belliard, J.-P., S., T., 2019. How effective are tidal marshes as nature-based shoreline protection throughout seasons? Limnol 64 (4), 1750–1762. https://doi.org/10.1002/LNO.11149.
Scrimshaw, M.D., Lester, J.N., 1997. Estimates of the inputs of polychlorinated biphenyls and organochlorine insecticides to the river Thames derived from the sediment record. Phil. Trans. R. Soc. A 355 (1722), 190–212. https://doi.org/10.1098/rsta.1997.0005.
Simon-Sánchez, L., Grelaud, M., Lorenz, C., Garcia-Orellana, J., Vianello, A., Liu, F., Vollertsen, J., Ziveri, P., 2022. Can a sediment core reveal the plastic age? Microplastic preservation in a coastal sedimentary record. Environ. Sci. Technol. 56 (23), 16780–16788. https://doi.org/10.1021/acs.est.2c04264.
Stead, J.L., Cundy, A.B., Hudson, M.D., Thompson, C.E.L., Williams, I.D., Russell, A.E., Pabortsava, K., 2020. Identification of tidal trapping of microplastics in a temperate salt marsh system using sea surface microlayer sampling. Sci. Rep. 10 (1), 14147. https://doi.org/10.1038/s41598-020-70306-5.
Thompson, R.C., Swan, S.H., Moore, C.J., Saal, F.S.V., 2009. Our plastic age. Philos. Trans. R. Soc. B 364 (1526). https://doi.org/10.1098/rstb.2009.0054.
Tibbetts, J., Krause, S., Lynch, I., Smith, G.H.S., 2018. Abundance, distribution, and drivers of microplastic contamination in urban river environments. Water 10 (11), 1597. https://doi.org/10.3390/w10111597.
Trusler, M.M., Moss-Hayes, V.L., Cook, S., Lomax, B.H., Vane, C.H., 2024. Microplastics pollution in sediments of the Thames and Medway estuaries, UK: organic matter associations and predominance of polyethylene. Mar. Pollut. Bull. 208 (116971). https://doi.org/10.1016/j.marpolbul.2024.116971.
Vane, C.H., Harrison, I., Kim, A.W., 2007. Polycyclic aromatic hydrocarbons (PAHs) and polychlorinated biphenyls (PCBs) in sediments from the Mersey estuary, U.K. Sci. Total Environ. 374 (1), 112–126. https://doi.org/10.1016/j.scitotenv.2006.12.036.
Vane, C.H., Beriro, D., Turner, G., 2015. Rise and fall of mercury (Hg) pollution in sediment cores of the Thames estuary, London, UK. Earth Environ. Sci. Trans. 105 (4), 285–296. https://doi.org/10.1017/S1755691015000158.
Vane, C.H., Lopes dos Santos, R.A., Kim, A.W., Moss-Hayes, V., Fordyce, F.M., Bearcock, J.M., 2017. Persistent organic pollutants (PAH, PCB, TPH) in freshwater, urban tributary and estuarine surface sediments of the river Clyde, Scotland, UK. Earth Environ. Sci. Trans. 108, 2–3. https://doi.org/10.1017/S1755691018000294.
Vane, C.H., Turner, G.H., Chenery, S.R., Richardson, M., Cave, M.C., Terrington, R., Gowing, C.J.B., Moss-Hayes, V., 2020a. Trends in heavy metals, polychlorinated biphenyls and toxicity from sediment cores of the inner river Thames estuary, London, UK. Environ. Sci.: Process Impacts 22, 364–380. https://doi.org/10.1039/C9EM00430K.
Vane, C.H., Kim, A.W., Moss-Hayes, V., Turner, G., Mills, K., Chenery, S.R., Barlow, T.S., Kemp, A.C., Engelhart, S.E., Hill, T.D., Horton, B.P., Brain, M., 2020b. Organic pollutants, heavy metals and toxicity in oil spill impacted salt marsh sediment cores,

Staten Island, New York City, USA. Mar. Pollut. Bull. 151, 110721. https://doi.org/10.1016/j.marpolbul.2019.110721.

Vane, C.H., Kim, A.W., Lopes dos Santos, R.A., Moss-Hayes, V., 2022. Contrasting sewage, emerging and persistent organic pollutants in sediment cores from the river Thames estuary, London, England, UK. Mar. Pollut. Bull. 175, 113340. https://doi.org/10.1016/j.marpolbul.2022.113340.

Williams, T.P., Bubb, J.M., Lester, J.N., 1994. Metal accumulation within salt marsh environments: a review. Mar. Pollut. Bull. 28 (5), 277–290. https://doi.org/10.1016/0025-326X(94)90152-X.

Willis, K.A., Eriksen, R., Wilcox, C., Hardesty, B.D., 2017. Microplastic distribution at different sediment depths in an urban estuary. Front. Mar. Sci. 4, 419. https://doi.org/10.3389/fmars.2017.00419.

Woodward, J., Li, J., Rothwell, J., Hurley, R., 2021. Acute riverine microplastic contamination due to avoidable releases of untreated wastewater. Nature Sustainability 4 (9), 793–802. https://doi.org/10.1038/s41893-021-00718-2.

Yao, W., Di, D., Wang, Z., Liao, Z., Huang, H., Mei, K., Dahlgren, R.A., Zhang, M., Shang, X., 2019. Micro- and macroplastic accumulation in a newly formed *Spartina alterniflora* colonized estuarine saltmarsh in Southeast China. Mar. Pollut. Bull. 149, 110636. https://doi.org/10.1016/j.marpolbul.2019.110636.

Zambrano, M.C., Pawlak, J.J., Daystar, J., Ankeny, M., Cheng, J.J., Venditti, R.A., 2019. Microfibers generated from the laundering of cotton, rayon and polyester sased fabrics and their aquatic biodegradation. Mar. Pollut. Bull. 142, 394–407. https://doi.org/10.1016/j.marpolbul.2019.02.062.